

On the precision of a data-driven estimate of  
the pseudoscalar-pole contribution to hadronic  
light-by-light scattering in the muon  $g - 2$

Andreas Nyffeler

Institute for Nuclear Physics  
Johannes Gutenberg Universität Mainz, Germany  
nyffeler@kph.uni-mainz.de

High-precision QCD at low energy  
Benasque, Spain  
August 7, 2015

# Outline

- Introduction
- Dispersive approach to HLbL
- Pion-pole contribution
  - 3-dim. integral representation, model independent weight functions
  - Contributions to  $a_{\mu}^{\text{HLbL};\pi^0}$  from different momentum regions
  - Impact of form factor uncertainties on  $a_{\mu}^{\text{HLbL};\pi^0}$
- Pole contributions from  $\eta$  and  $\eta'$ 
  - Weight functions
  - Contributions from different momentum regions
  - Impact of form factor uncertainties
- Conclusions and Outlook

## Muon $g - 2$ : current status

Contribution	$a_\mu \times 10^{11}$	Reference
QED (leptons)	116 584 718.853 $\pm$ 0.036	Aoyama et al. '12
Electroweak	153.6 $\pm$ 1.0	Gnendiger et al. '13
HVP: LO	6907.5 $\pm$ 47.2	Jegerlehner + Szafron '11
NLO	-100.3 $\pm$ 2.2	Jegerlehner + Szafron '11
NNLO	12.4 $\pm$ 0.1	Kurz et al. '14
HLbL	116 $\pm$ 40	Jegerlehner + AN '09
NLO	3 $\pm$ 2	Colangelo et al. '14
Theory (SM)	116 591 811 $\pm$ 62	
Experiment	116 592 089 $\pm$ 63	Bennett et al. '06
Experiment - Theory	278 $\pm$ 88	3.1 $\sigma$

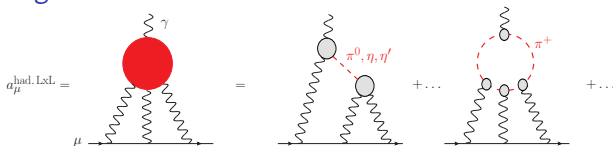
HVP: Hadronic vacuum polarization

HLbL: Hadronic light-by-light scattering

Other estimate:  $a_\mu^{\text{HLbL}} = (105 \pm 26) \times 10^{-11}$  (Prades, de Rafael, Vainshtein '09).

Discrepancy a sign of New Physics ? Hadronic uncertainties need to be better controlled in order to fully profit from future  $g - 2$  experiments with  $\delta a_\mu = 16 \times 10^{-11}$ . Way forward for HVP seems clear with more precise measurements for  $\sigma(e^+e^- \rightarrow \text{hadrons})$ , not so obvious how to improve HLbL.

## HLbL in muon $g - 2$



- Only model calculations so far: large uncertainties, difficult to control.
- Frequently used estimates:

$$a_{\mu}^{\text{HLbL}} = (105 \pm 26) \times 10^{-11} \quad (\text{Prades, de Rafael, Vainshtein '09})$$

$$a_{\mu}^{\text{HLbL}} = (116 \pm 40) \times 10^{-11} \quad (\text{AN '09; Jegerlehner, AN '09})$$

Based almost on same input: calculations by various groups using different models for individual contributions. Error estimates are mostly guesses !

- Need much better understanding of complicated hadronic dynamics to get reliable error estimate of  $\pm 20 \times 10^{-11}$  ( $\sim 20\%$ ) (or even 10%).
- Recent new proposal: Colangelo et al. '14, '15; Pauk, Vanderhaeghen '14: use dispersion relations (DR) to connect contribution to HLbL from light pseudoscalars to in principle measurable form factors and cross-sections:

$$\gamma^* \gamma^* \rightarrow \pi^0, \eta, \eta'$$

$$\gamma^* \gamma^* \rightarrow \pi\pi$$

Could connect HLbL uncertainty to exp. measurement errors, like HVP.

- Maybe in future: HLbL from Lattice QCD. First steps: Blum et al. '05, ..., '14, '15. Work started by Mainz group (talk by Jeremy Green).

## Data-driven approach to HLbL using dispersion relations (DR)

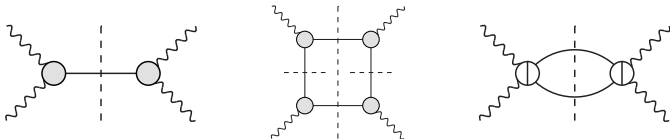
- Strategy: Split contributions to HLbL into two parts:
  - I: **Data-driven evaluation using DR** (hopefully numerically dominant):
    - (1)  $\pi^0, \eta, \eta'$  poles
    - (2)  $\pi\pi$  intermediate state
  - II: **Model dependent evaluation** (hopefully numerically subdominant):
    - (1) Axial vectors ( $3\pi$ -intermediate state), ...
    - (2) Quark-loop, matching with pQCD

**Error goals:** Part I: 10% precision (data driven), Part II: 30% precision.

To achieve overall error of about 20% ( $\delta a_\mu^{\text{HLbL}} = 20 \times 10^{-11}$ ).

More efforts needed to get down to 10% overall precision !

- Colangelo et al.:  
Classify intermediate states in four-point function. Then project onto  $g - 2$ .



- Pauk, Vanderhaeghen:  
Write DR directly for Pauli form factor  $F_2(k^2)$ .

## Pseudoscalar contribution to HLbL

- Most calculations for neutral pion and all light pseudoscalars  $\pi^0, \eta, \eta'$  agree at level of 15%, but full range of estimates is much larger:

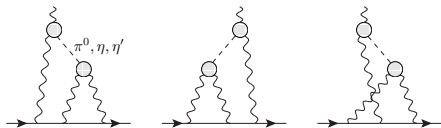
$$a_{\mu}^{\text{HLbL};\pi^0} = (50 - 80) \times 10^{-11} = (65 \pm 15) \times 10^{-11} (\pm 23\%)$$

$$a_{\mu}^{\text{HLbL};\text{P}} = (59 - 114) \times 10^{-11} = (87 \pm 27) \times 10^{-11} (\pm 31\%)$$

**Note:** not always clear, what is calculated, e.g. for  $\pi^0$ : pion-pole (as in DR approach), pion-pole with constant form factor at external vertex (Melnikov, Vainshtein '04), pion-exchange with off-shell form factors.

- This talk:** try to study precision which could be reached with a data-driven estimate of the pseudoscalar-pole contribution to HLbL.
- Show relevant momentum regions where data on doubly off-shell form factor  $\mathcal{F}_{\pi^0\gamma^*\gamma^*}(-Q_1^2, -Q_2^2)$  will be needed from direct experimental measurements, via a DR for form factor itself (Hoferichter et al. '14) or from Lattice QCD to better control this numerically dominant contribution to HLbL and its uncertainty.
- Present impact on precision of  $a_{\mu}^{\text{HLbL};\text{P}}$  based on estimated experimental uncertainties of  $\mathcal{F}_{\pi^0\gamma^*\gamma^*}(-Q_1^2, -Q_2^2)$  using results from Monte Carlo simulation for BES III (Mainz group: Denig, Redmer, Wasser).
- Similar to "pie-charts" for  $a_{\mu}^{\text{HVP}}$  and its uncertainty  $\delta a_{\mu}^{\text{HVP}}$  as function of centre-of-mass energy  $\sqrt{s}$ .

## Pion-pole contribution (Knecht, AN '02)



$$a_{\mu}^{\text{HLbL};\pi^0} = \left(\frac{\alpha}{\pi}\right)^3 \left[ a_{\mu}^{\text{HLbL};\pi^0(1)} + a_{\mu}^{\text{HLbL};\pi^0(2)} \right]$$

$$a_{\mu}^{\text{HLbL};\pi^0(1)} = \int \frac{d^4 q_1}{(2\pi)^4} \frac{d^4 q_2}{(2\pi)^4} \frac{1}{q_1^2 q_2^2 (q_1 + q_2)^2 [(p + q_1)^2 - m_{\mu}^2] [(p - q_2)^2 - m_{\mu}^2]} \\ \times \frac{\mathcal{F}_{\pi^0 \gamma^* \gamma^*}(q_1^2, (q_1 + q_2)^2)}{q_2^2 - m_{\pi}^2} \frac{\mathcal{F}_{\pi^0 \gamma^* \gamma^*}(q_2^2, 0)}{\tilde{T}_1(q_1, q_2; p)}$$

$$a_{\mu}^{\text{HLbL};\pi^0(2)} = \int \frac{d^4 q_1}{(2\pi)^4} \frac{d^4 q_2}{(2\pi)^4} \frac{1}{q_1^2 q_2^2 (q_1 + q_2)^2 [(p + q_1)^2 - m_{\mu}^2] [(p - q_2)^2 - m_{\mu}^2]} \\ \times \frac{\mathcal{F}_{\pi^0 \gamma^* \gamma^*}(q_1^2, q_2^2)}{(q_1 + q_2)^2 - m_{\pi}^2} \frac{\mathcal{F}_{\pi^0 \gamma^* \gamma^*}((q_1 + q_2)^2, 0)}{\tilde{T}_2(q_1, q_2; p)}$$

where  $p^2 = m_{\mu}^2$  and the external photon has now zero four-momentum (soft photon).

Pion-pole contribution determined by measurable pion transition form factor  $\mathcal{F}_{\pi^0 \gamma^* \gamma^*}(q_1^2, q_2^2)$  (on-shell pion, one or two off-shell photons). Currently, only single-virtual TFF  $\mathcal{F}_{\pi^0 \gamma^* \gamma^*}(-q^2, 0)$  has been measured by CELLO, CLEO, BABAR, Belle (mostly) for spacelike momenta. Analysis ongoing at BES III, measurement planned at KLOE-2. Measurement of double-virtual form factor planned at BES III. Analogously for  $\eta, \eta'$ -pole contributions.

### 3-dimensional integral representation (Jegerlehner, AN '09)

$$a_{\mu}^{\text{HLbL};\pi^0} = \left(\frac{\alpha}{\pi}\right)^3 \left[ a_{\mu}^{\text{HLbL};\pi^0(1)} + a_{\mu}^{\text{HLbL};\pi^0(2)} \right]$$

$$a_{\mu}^{\text{HLbL};\pi^0(1)} = \int_0^{\infty} dQ_1 \int_0^{\infty} dQ_2 \int_{-1}^1 dt w_1(Q_1, Q_2, t) \mathcal{F}_{\pi^0\gamma^*\gamma^*}(-Q_1^2, -(Q_1+Q_2)^2) \mathcal{F}_{\pi^0\gamma^*\gamma^*}(-Q_2^2, 0)$$

$$a_{\mu}^{\text{HLbL};\pi^0(2)} = \int_0^{\infty} dQ_1 \int_0^{\infty} dQ_2 \int_{-1}^1 dt w_2(Q_1, Q_2, t) \mathcal{F}_{\pi^0\gamma^*\gamma^*}(-Q_1^2, -Q_2^2) \mathcal{F}_{\pi^0\gamma^*\gamma^*}(-(Q_1+Q_2)^2, 0)$$

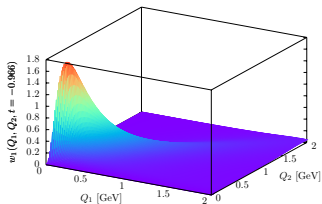
$$w_1(Q_1, Q_2, t) = \left(-\frac{2\pi}{3}\right) \sqrt{1-t^2} \frac{Q_1^3 Q_2^3}{Q_2^2 + m_{\pi}^2} l_1(Q_1, Q_2, t)$$

$$w_2(Q_1, Q_2, t) = \left(-\frac{2\pi}{3}\right) \sqrt{1-t^2} \frac{Q_1^3 Q_2^3}{(Q_1 + Q_2)^2 + m_{\pi}^2} l_2(Q_1, Q_2, t)$$

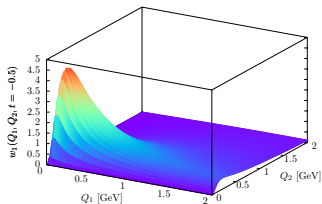
- After Wick rotation:  $Q_1, Q_2$  are Euclidean (spacelike) four-momenta. Integrals run over the lengths of the four-vectors with  $Q_i \equiv |(Q_i)_{\mu}|, i = 1, 2$  and angle  $\theta$  between them:  $Q_1 \cdot Q_2 = Q_1 Q_2 \cos \theta, t = \cos \theta$ .
- Separation of generic kinematics described by model-independent weight functions  $w_{1,2}(Q_1, Q_2, t)$  and double-virtual form factors  $\mathcal{F}_{\pi^0\gamma^*\gamma^*}(-Q_1^2, -Q_2^2)$  which can in principle be measured.
- $w_{1,2}(Q_1, Q_2, t)$ : dimensionless.  $w_2(Q_1, Q_2, t)$  symmetric under  $Q_1 \leftrightarrow Q_2$ .
- $w_{1,2}(Q_1, Q_2, t) \rightarrow 0$  for  $Q_{1,2} \rightarrow 0$ .  $w_{1,2}(Q_1, Q_2, t) \rightarrow 0$  for  $t \rightarrow \pm 1$ .

# Relevant momentum regions in $a_{\mu}^{\text{HLbL};\pi^0}$

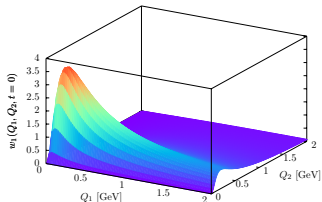
Weight function  $w_1(Q_1, Q_2, t)$



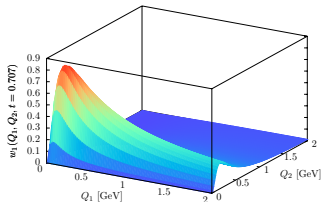
$t = -0.966, \quad \theta = 165^\circ$



$t = -0.5, \quad \theta = 120^\circ$



$t = 0, \quad \theta = 90^\circ$



$t = 0.707, \quad \theta = 45^\circ$

**Low momentum region most important.** Peak around  $Q_1 \sim 0.2$  GeV,  $Q_2 \sim 0.15$  GeV.

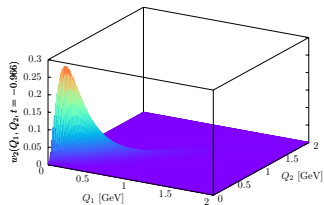
Despite the appearance in the plots, the slopes along the two axis and along the diagonal (at  $Q_1 = Q_2 = 0$ ) vanish.

For  $t > -0.85$  ( $\theta < 150^\circ$ ) a ridge develops along  $Q_1$  direction for  $Q_2 \sim 0.2$  GeV.

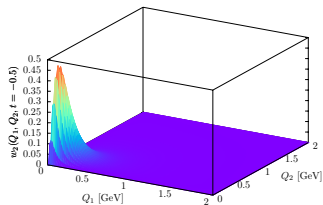
Leads for constant form factor to a divergence  $\ln^2 \Lambda$  for some momentum cutoff  $\Lambda$ .

Realistic form factor falls off for large  $Q_i$  and integral  $a_{\mu}^{\text{HLbL};\pi^0(1)}$  will be convergent.

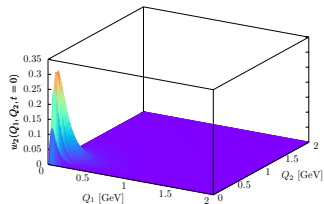
## Weight function $w_2(Q_1, Q_2, t)$



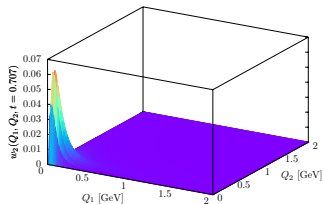
$$t = -0.966, \quad \theta = 165^\circ$$



$$t = -0.5, \quad \theta = 120^\circ$$



$$t = 0, \quad \theta = 90^\circ$$



$$t = 0.707, \quad \theta = 45^\circ$$

$w_2$  is about a factor 10 smaller than  $w_1$  and there is **no ridge** in one direction. Note that  $w_2(Q_1, Q_2, t)$  is symmetric under  $Q_1 \leftrightarrow Q_2$ . Peak for  $Q_1 = Q_2 \sim 0.15$  GeV for  $t$  near  $-1$ , peak moves to lower values  $Q_1 = Q_2 = 0.04$  GeV for  $t$  near 1.

Again the slopes along the two axis and along the diagonal (at  $Q_1 = Q_2 = 0$ ) vanish.

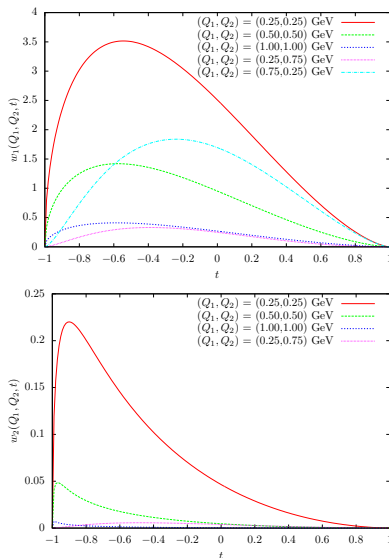
Even for **constant form factor**, one obtains finite result:  $\left(\frac{\alpha}{\pi}\right)^3 a_{\mu;WZW}^{\text{HLbL};\pi^0(2)} \sim 2.5 \times 10^{-11}$

## Locations and values of maxima of $w_{1,2}(Q_1, Q_2, t)$

$\theta$ ( $t = \cos \theta$ )	Max. $w_1$	$Q_1$ [GeV]	$Q_2$ [GeV]	Max. $w_2$	$Q_1 = Q_2$ [GeV]
175° (-0.996)	0.592	0.163	0.163	0.100	0.142
165° (-0.966)	1.734	0.164	0.162	0.277	0.132
150° (-0.866)	3.197	0.166	0.158	0.441	0.114
135° (-0.707)	4.176	0.171	0.153	0.494	0.099
120° (-0.5)	4.559	0.176	0.146	0.471	0.087
105° (-0.259)	4.349	0.182	0.139	0.403	0.078
90° (0.0)	3.664	0.187	0.130	0.312	0.070
75° (0.259)	2.702	0.189	0.122	0.218	0.063
60° (0.5)	1.691	0.187	0.114	0.132	0.057
45° (0.707)	0.840	0.180	0.106	0.064	0.050
30° (0.866)	0.283	0.168	0.099	0.021	0.043
15° (0.966)	0.0385	0.154	0.092	0.0027	0.037
5° (0.996)	0.0015	0.147	0.089	0.000092	0.037

- **Global maximum of  $w_1(Q_1, Q_2, t) = 4.563$**   
 $(Q_1 = 0.177 \text{ GeV}, Q_2 = 0.145 \text{ GeV}, \theta = 118.1^\circ (t = -0.471))$
- **Global minimum of  $w_1(Q_1, Q_2, t) = -0.0044$**   
 $(Q_1 = 0.118 \text{ GeV}, Q_2 = 1.207 \text{ GeV}, \theta = 45.7^\circ (t = 0.698))$
- **Global maximum of  $w_2(Q_1, Q_2, t) = 0.495$**   
 $(Q_1 = Q_2 = 0.097 \text{ GeV and } \theta = 133.1^\circ (t = -0.684))$

Variation of  $w_{1,2}(Q_1, Q_2, t)$  with  $t = \cos \theta$  for selected  $Q_1, Q_2$



Strong enhancement for  $Q_1 = Q_2$  for negative  $t$ , when the original four-vectors  $(Q_1)_\mu$  and  $(Q_2)_\mu$  become more antiparallel. For  $Q_1 = Q_2$  both weight functions have infinite slope at  $t = -1$ . Overall, weight functions get smaller for larger  $Q_i > 0.5$  GeV.

## For illustration: LMD+V and VMD models

- Since the integral  $a_{\mu}^{\text{HLbL};\pi^0(1)}$  is divergent without form factors, we take two simple models for illustration to see where are the relevant momentum regions in the integral.
- Of course, in the end, the models have to be replaced by experimental data on the doubly-virtual form factor  $\mathcal{F}_{\pi^0\gamma^*\gamma^*}(-Q_1^2, -Q_2^2)$ .
- LMD+V model (Lowest Meson Dominance + V) is a generalization of Vector Meson Dominance (VMD) in the framework of large- $N_C$  QCD, which respects (some) short-distance constraints from the operator product expansion (OPE).
- Main difference is doubly-virtual case: VMD model violates OPE, falls off too fast:

$$\mathcal{F}_{\pi^0\gamma^*\gamma^*}^{\text{VMD}}(-Q^2, -Q^2) \sim \frac{1}{Q^4} \quad \text{for large } Q^2$$

$$\mathcal{F}_{\pi^0\gamma^*\gamma^*}^{\text{LMD+V}}(-Q^2, -Q^2) \sim \mathcal{F}_{\pi^0\gamma^*\gamma^*}^{\text{OPE}}(-Q^2, -Q^2) \sim \frac{1}{Q^2} \quad \text{for large } Q^2$$

# Contributions to $a_{\mu}^{\text{HLbL};\pi^0}$ from different momentum regions

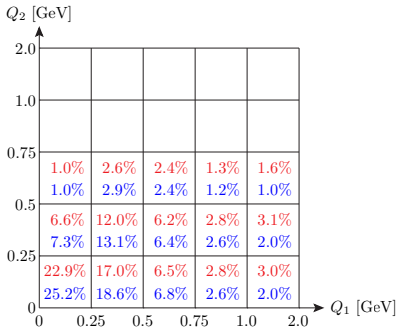
$$a_{\mu;\text{LMD+V}}^{\text{HLbL};\pi^0} = 62.9 \times 10^{-11}$$

$$a_{\mu;\text{VMD}}^{\text{HLbL};\pi^0} = 57.0 \times 10^{-11}$$

Integrate over individual momentum bins:

$$\int_{Q_{1,\min}}^{Q_{1,\max}} dQ_1 \int_{Q_{2,\min}}^{Q_{2,\max}} dQ_2 \int_{-1}^1 dt$$

Contribution of individual bins to total:



Bin sizes vary. No entry: contribution  $< 1\%$ .

Asymmetry in  $(Q_1, Q_2)$ -plane with larger contributions below diagonal reflects ridge-like structure in dominant  $w_1(Q_1, Q_2, t)$ .

Pion-pole contribution  $a_{\mu}^{\text{HLbL};\pi^0} \times 10^{11}$  for LMD+V and VMD form factors obtained with momentum cutoff  $\Lambda$  (integration over square). In brackets, relative contribution of the total obtained with  $\Lambda = 20$  GeV.

$\Lambda$ [GeV]	LMD+V	VMD
0.25	14.4 (22.9%)	14.4 (25.2%)
0.5	36.8 (58.5%)	36.6 (64.2%)
0.75	48.5 (77.1%)	47.7 (83.8%)
1.0	54.1 (86.0%)	52.6 (92.3%)
1.5	58.8 (93.4%)	55.8 (97.8%)
2.0	60.5 (96.2%)	56.5 (99.2%)
5.0	62.5 (99.4%)	56.9 (99.9%)
20.0	62.9 (100%)	57.0 (100%)

Region below  $\Lambda = 0.5$  GeV gives more than half of the contribution: 59% for LMD+V, 64% for VMD.

Bulk of result below  $\Lambda = 1$  GeV: 86% for LMD+V, 92% for VMD.

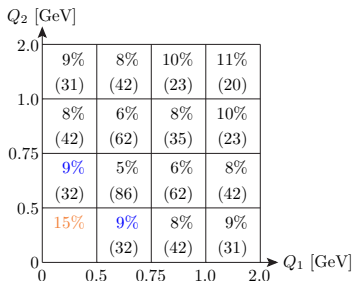
VMD: faster fall-off, contributions more concentrated at lower momenta compared to LMD+V.

## Impact of form factor uncertainties

Very rough description of measurement errors in the **double-virtual form factor**

$$\mathcal{F}_{\pi^0\gamma^*\gamma^*}(-Q_1^2, -Q_2^2) \\ \rightarrow \mathcal{F}_{\pi^0\gamma^*\gamma^*}(-Q_1^2, -Q_2^2) (1 + \delta_2(Q_1, Q_2))$$

where the momentum dependent errors  $\delta_2(Q_1, Q_2)$  are assumed as follows:



Note the unequal bin sizes ! In brackets: number of MC events  $N_i$  in each bin  $\sim \sigma \sim \mathcal{F}_{\pi^0\gamma^*\gamma^*}^2 \Rightarrow \delta\mathcal{F}_{\pi^0\gamma^*\gamma^*} = \sqrt{N_i}/(2N_i)$  (total: 600 events). For **lowest bin, assumed error** (“extrapolation” from boundary values), no events in simulation (detector acceptance).

Monte Carlo simulations for reaction  $e^+e^- \rightarrow e^+e^-\gamma^*\gamma^* \rightarrow e^+e^-\pi^0$  at BES III (Mainz group) based on LMD+V model in EKHARA (Czyż, Ivashyn '11)

Number of events and corresponding precision for  $\mathcal{F}_{\pi^0\gamma^*\gamma^*}(-Q_1^2, -Q_2^2)$  should be achievable with current data set at BES III plus a few more years of data taking.

For the **single-virtual form factor** we proceed in a similar way

$$\mathcal{F}_{\pi^0\gamma^*\gamma^*}(-Q^2, 0) \\ \rightarrow \mathcal{F}_{\pi^0\gamma^*\gamma^*}(-Q^2, 0) (1 + \delta_1(Q))$$

where we assumed the following momentum dependent errors for  $\delta_1(Q)$ :

Momentum range [GeV]	$\delta_1(Q)$
$0 \leq Q < 0.5$	5%
$0.5 \leq Q < 2$	7.5%
$2 \leq Q$	12.5%

Based on measurements by CLEO and ongoing analysis by BES III. For **lowest bin, assumed error**. Use of a dispersion relation for form factor could help at low energies (Hoferichter et al. '14).

## Impact of form factor uncertainties (continued)

LMD+V model [VMD model] (relative errors very similar)

$$a_{\mu}^{\text{HLbL};\pi^0}_{\text{LMD+V}} = 62.9 \times 10^{-11} \quad \left[ a_{\mu}^{\text{HLbL};\pi^0}_{\text{VMD}} = 57.0 \times 10^{-11} \right]$$

$\delta a_{\mu}^{\text{HLbL};\pi^0} \times 10^{11}$	Relative error	Comment
$+11.5$ $[-10.6]$ $[+10.4]$ $[-9.6]$	$+18.2\%$ $[-16.8\%]$ $[+18.3\%]$ $[-16.8\%]$	Given $\delta_1, \delta_2$
$+2.7$ $[-2.6]$ $[+2.5]$ $[-2.4]$	$+4.3\%$ $[-4.2\%]$ $[+4.4\%]$ $[-4.2\%]$	Bin $Q < 0.5$ GeV in $\delta_1 = 5\%$ , rest: $\delta_{1,2} = 0$
$+0.7$ $[-0.7]$ $[+0.6]$ $[-0.5]$	$+1.2\%$ $[-1.0\%]$ $[+1.0\%]$ $[-0.9\%]$	Bins $Q \geq 0.5$ GeV in $\delta_1$ as given, rest: $\delta_{1,2} = 0$
$+5.2$ $[-5.2]$ $[+5.2]$ $[-5.1]$	$+8.3\%$ $[-8.2\%]$ $[+9.2\%]$ $[-9.0\%]$	Bin $Q_{1,2} < 0.5$ GeV in $\delta_2 = 15\%$ , rest: $\delta_{1,2} = 0$
$+2.5$ $[-2.4]$ $[+1.8]$ $[-1.7]$	$+3.9\%$ $[-3.8\%]$ $[+3.2\%]$ $[-3.0\%]$	Bins $Q_{1,2} \geq 0.5$ GeV in $\delta_2$ as given, rest: $\delta_{1,2} = 0$
$+10.3$ $[-9.6]$ $[+9.3]$ $[-8.7]$	$+16.3\%$ $[-15.3\%]$ $[+16.3\%]$ $[-15.3\%]$	Given $\delta_1, \delta_2$ , but lowest bin in $\delta_1$ : $5\% \rightarrow 3\%$
$+8.7$ $[-8.1]$ $[+7.7]$ $[-7.1]$	$+13.9\%$ $[-12.9\%]$ $[+13.5\%]$ $[-12.5\%]$	Given $\delta_1, \delta_2$ , but lowest bin in $\delta_2$ : $15\% \rightarrow 7.5\%$
$+8.5$ $[-7.9]$ $[+7.4]$ $[-6.9]$	$+13.5\%$ $[-12.5\%]$ $[+13.0\%]$ $[-12.1\%]$	In addition: bins in $\delta_2$ close to lowest bin $9\% \rightarrow 5\%$

For LMD+V FF [VMD FF], region  $Q_{1,2} < 0.5$  GeV gives  $59\%$  [ $64\%$ ] to total.

In order to reach goal of 10% error for  $a_{\mu}^{\text{HLbL};\pi^0}$ , it would help, if one could measure double-virtual TFF in region  $Q_{1,2} < 0.5$  GeV, constrain it using DR or with informations from Lattice QCD.

Recall model calculations:  $a_{\mu}^{\text{HLbL};\pi^0} = (50 - 80) \times 10^{-11} = (65 \pm 15) \times 10^{-11}$  ( $\pm 23\%$ ).

## Pole contributions from $\eta$ and $\eta'$

Only dependence on pseudoscalars appears in weight functions through pseudoscalar mass  $m_P$  in propagators:

$$\text{In weight function } w_1(Q_1, Q_2, t) : \frac{1}{Q_2^2 + m_P^2}$$

$$\text{In weight function } w_2(Q_1, Q_2, t) : \frac{1}{(Q_1 + Q_2)^2 + m_P^2} = \frac{1}{Q_1^2 + 2Q_1 Q_2 t + Q_2^2 + m_P^2}$$

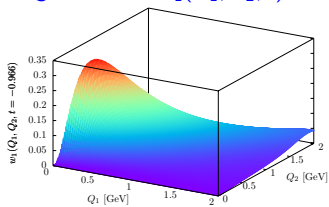
Two effects:

1. Shifts the relevant momentum regions (peaks, ridges) to higher momenta for  $\eta$  compared to  $\pi^0$  and even higher for  $\eta'$ .
2. Leads to suppression in absolute size of the weight functions due to larger masses in the propagators:

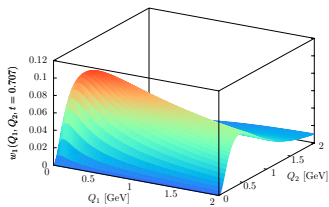
$$w_1|_{\eta} \approx \frac{1}{6} w_1|_{\pi^0}$$
$$w_1|_{\eta'} \approx \frac{1}{2.5} w_1|_{\eta}$$

# Weight functions for $\eta$

Weight function  $w_1(Q_1, Q_2, t)$

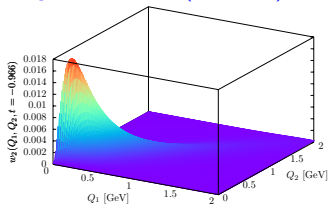


$t = -0.966, \quad \theta = 165^\circ$

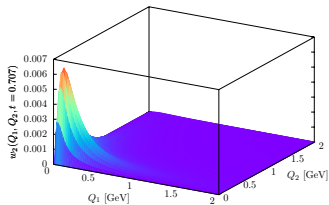


$t = 0.707, \quad \theta = 45^\circ$

Weight function  $w_2(Q_1, Q_2, t)$



$t = -0.966, \quad \theta = 165^\circ$



$t = 0.707, \quad \theta = 45^\circ$

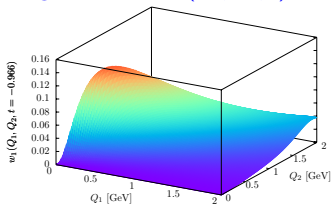
Peaks and ridges have broadened compared to  $\pi^0$ .

Peak for  $w_1$  around  $Q_1 \sim 0.32 - 0.37$  GeV,  $Q_2 \sim 0.22 - 0.33$  GeV.  $w_2$  about a factor 20 smaller than  $w_1$ . Peak for  $w_2$  around  $Q_1 = Q_2 \sim 0.14$  GeV for  $t$  near  $-1$ , moves down to  $Q_1 = Q_2 = 0.06$  GeV for  $t$  near 1.

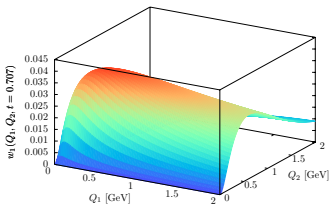
$w_2$ : finite result for constant form factor  $\left(\frac{\alpha}{\pi}\right)^3 a_{\mu;WZW}^{\text{HLbL};\eta(2)} = 0.78 \times 10^{-11}$

# Weight functions for $\eta'$

Weight function  $w_1(Q_1, Q_2, t)$

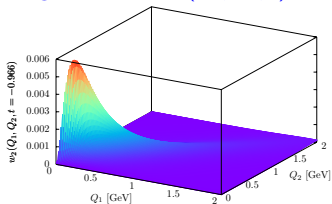


$t = -0.966, \quad \theta = 165^\circ$

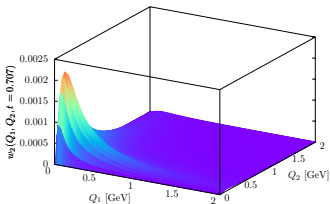


$t = 0.707, \quad \theta = 45^\circ$

Weight function  $w_2(Q_1, Q_2, t)$



$t = -0.966, \quad \theta = 165^\circ$



$t = 0.707, \quad \theta = 45^\circ$

Peaks and ridges have broadened even more.

Peak for  $w_1$  around  $Q_1 \sim 0.41 - 0.51$  GeV,  $Q_2 \sim 0.31 - 0.43$  GeV.  $w_2$  about a factor 20 smaller than  $w_1$ . Peak for  $w_2$  around  $Q_1 = Q_2 \sim 0.14$  GeV for  $t$  near  $-1$ , moves down to  $Q_1 = Q_2 = 0.07$  GeV for  $t$  near 1.

$w_2$ : finite result for constant form factor  $\left(\frac{\alpha}{\pi}\right)^3 a_{\mu;WZW}^{\text{HLbL};\eta'}(2) = 0.65 \times 10^{-11}$

# Locations of maxima of $w_{1,2}(Q_1, Q_2, t)$ for $\eta$ (top) and $\eta'$ (bottom)

$\theta$ ( $t = \cos \theta$ )	Max. $w_1$	$Q_1$ [GeV]	$Q_2$ [GeV]	Max. $w_2$	$Q_1 = Q_2$ [GeV]
175° (-0.996)	0.117	0.328	0.328	0.0061	0.143
165° (-0.966)	0.341	0.327	0.327	0.018	0.142
150° (-0.866)	0.616	0.325	0.323	0.032	0.137
135° (-0.707)	0.778	0.323	0.317	0.041	0.131
120° (-0.5)	0.809	0.322	0.308	0.044	0.123
105° (-0.259)	0.729	0.323	0.296	0.040	0.114
90° (0.0)	0.575	0.328	0.282	0.032	0.106
75° (0.259)	0.395	0.336	0.267	0.023	0.096
60° (0.5)	0.231	0.346	0.253	0.014	0.087
45° (0.707)	0.107	0.356	0.241	0.0063	0.077
30° (0.866)	0.034	0.363	0.231	0.0019	0.067
15° (0.966)	0.0044	0.367	0.225	0.00023	0.063
5° (0.996)	0.00017	0.368	0.224	$8 \times 10^{-6}$	0.065
175° (-0.996)	0.049	0.434	0.434	0.0020	0.143
165° (-0.966)	0.142	0.432	0.433	0.0059	0.142
150° (-0.866)	0.255	0.427	0.430	0.011	0.139
135° (-0.707)	0.320	0.419	0.423	0.014	0.134
120° (-0.5)	0.330	0.413	0.412	0.015	0.128
105° (-0.259)	0.293	0.412	0.397	0.014	0.120
90° (0.0)	0.227	0.418	0.378	0.011	0.112
75° (0.259)	0.154	0.431	0.358	0.0079	0.102
60° (0.5)	0.088	0.451	0.340	0.0047	0.092
45° (0.707)	0.041	0.472	0.326	0.0022	0.082
30° (0.866)	0.013	0.491	0.315	0.00066	0.072
15° (0.966)	0.0017	0.504	0.309	0.000079	0.067
5° (0.996)	0.000062	0.508	0.307	$3 \times 10^{-6}$	0.070

# Contributions to $a_{\mu}^{\text{HLbL};\eta}$ and $a_{\mu}^{\text{HLbL};\eta'}$ from different momentum regions

Use VMD model with adapted parameter  $F_P$  to describe  $\Gamma(P \rightarrow \gamma\gamma)$  and  $M_V$  from fit of  $\mathcal{F}_{P\gamma^*\gamma^*}(-Q^2, 0)$  to CLEO data:

$$F_{\eta} = 93.0 \text{ MeV}, \quad M_V = 775 \text{ MeV}$$

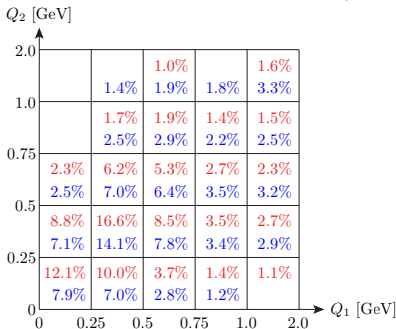
$$F_{\eta'} = 74.0 \text{ MeV}, \quad M_V = 859 \text{ MeV}$$

One obtains (Knecht, AN '02):

$$a_{\mu;\text{VMD}}^{\text{HLbL};\eta} = 14.5 \times 10^{-11}$$

$$a_{\mu;\text{VMD}}^{\text{HLbL};\eta'} = 12.5 \times 10^{-11}$$

Contribution of individual bins to total (bin sizes vary; no entry: contribution < 1%):



Pole contributions  $a_{\mu}^{\text{HLbL};\eta} \times 10^{11}$  and  $a_{\mu}^{\text{HLbL};\eta'} \times 10^{11}$  with the VMD form factor obtained with a momentum cutoff  $\Lambda$ . In brackets, relative contribution of the total obtained with  $\Lambda = 20 \text{ GeV}$ .

$\Lambda$ [GeV]	$\eta$	$\eta'$
0.25	1.8 (12.1%)	1.0 (7.9%)
0.5	6.9 (47.5%)	4.5 (36.1%)
0.75	10.7 (73.4%)	7.8 (62.5%)
1.0	12.6 (86.6%)	9.9 (79.1%)
1.5	14.0 (96.1%)	11.7 (93.1%)
2.0	14.3 (98.6%)	12.2 (97.4%)
5.0	14.5 (100%)	12.5 (99.9%)
20.0	14.5 (100%)	12.5 (100%)

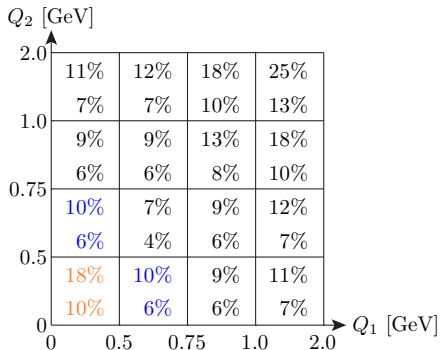
Region below  $\Lambda = 0.25 \text{ GeV}$  gives very small contribution to total: 12% for  $\eta$ , 8% for  $\eta'$ .

Region below  $\Lambda = 0.5 \text{ GeV}$  gives: 48% for  $\eta$ , 36% for  $\eta'$ .

Bulk of result below  $\Lambda = 1.5 \text{ GeV}$ : 96% for  $\eta$ , 93% for  $\eta'$ .

## Impact of form factor uncertainties

The momentum dependent errors  $\delta_2(Q_1, Q_2)$  are assumed as follows:



Top line in bin:  $\eta$ -meson (total: 345 events).

Bottom line:  $\eta'$ -meson (total: 902 events).

For **lowest bin, assumed error** ("extrapolation" from boundary values), no events in simulation (detector acceptance).

Note again the unequal bin sizes.

Monte Carlo simulations for BES III (Mainz group) based on VMD model in EKHARA (Czyż, Ivashyn '11)

Number of events and corresponding precision for  $\mathcal{F}_{P\gamma^*\gamma^*}(-Q_1^2, -Q_2^2)$  should be achievable with current data set plus a few more years of data taking, although the separation of signal and background will be more difficult for  $\eta$  and  $\eta'$  than for the pion.

For simplicity, for the **single-virtual form factor** we assume the same errors  $\delta_1(Q)$  as for the pion.

## Impact of form factor uncertainties (continued)

VMD model (for illustration)

$$a_{\mu; \text{VMD}}^{\text{HLbL}; \eta} = 14.5 \times 10^{-11} \left[ a_{\mu; \text{VMD}}^{\text{HLbL}; \eta'} = 12.5 \times 10^{-11} \right]$$

$\delta a_{\mu}^{\text{HLbL}; \eta[\eta']} \times 10^{11}$	Relative error	Comment
+3.1 [+1.9] -2.9 [-1.8]	+21.6% [+15.2%] -19.8% [-14.0%]	Given $\delta_1, \delta_2$
+0.5 [+0.4] -0.5 [-0.3]	+3.5% [+2.8%] -3.3% [-2.7%]	Bin $Q < 0.5$ GeV in $\delta_1 = 5\%$ , rest: $\delta_{1,2} = 0$
+0.4 [+0.4] -0.3 [-0.4]	+2.4% [+3.4%] -2.3% [-3.3%]	Bins $Q \geq 0.5$ GeV in $\delta_1$ as given, rest: $\delta_{1,2} = 0$
+1.2 [+0.4] -1.2 [-0.4]	+8.1% [+3.4%] -7.9% [-3.3%]	Bin $Q_{1,2} < 0.5$ GeV: $\delta_2 = 18\%[10\%]$ , rest: $\delta_{1,2} = 0$
+1.0 [+0.6] -1.0 [-0.6]	+6.9% [+5.1%] -6.8% [-5.0%]	Bins $Q_{1,2} \geq 0.5$ GeV in $\delta_2$ as given, rest: $\delta_{1,2} = 0$
+2.9 [+1.8] -2.7 [-1.6]	+20.0% [+14.0%] -18.6% [-13.0%]	Given $\delta_1, \delta_2$ , lowest bin in $\delta_1$ : $5\% \rightarrow 3\%$
+2.5 [+1.7] -2.3 [-1.6]	+17.4% [+13.4%] -16.0% [-12.4%]	Given $\delta_1, \delta_2$ , lowest bin in $\delta_2$ : $18\%[10\%] \rightarrow 9\%[5\%]$
+2.5 [+1.6] -2.3 [-1.5]	+16.9% [+13.0%] -15.5% [-12.1%]	<b>In addition:</b> bins in $\delta_2$ with $10\%[6\%] \rightarrow 7\%[4\%]$

For  $\eta$  [ $\eta'$ ], region  $Q_{1,2} < 0.5$  GeV gives  $48\%$  [ $36\%$ ] to total.

In order to reach **goal of 10% error** for  $a_{\mu}^{\text{HLbL}; \eta}$ , it would help, if one could measure double-virtual TFF in region  $Q_{1,2} < 0.5$  GeV. For  $a_{\mu}^{\text{HLbL}; \eta'}$ , information for  $0.5 \leq Q_{1,2} \leq 1$  GeV would be helpful.

## Conclusions and Outlook

- Started from 3-dimensional integral representation for pseudoscalar-pole contribution  $a_{\mu}^{\text{HLbL};\text{P}}$  derived in Jegerlehner, AN '09.
- Separates the generic kinematics with model-independent weight functions  $w_{1,2}(Q_1, Q_2, t)$  from doubly-virtual form factors  $\mathcal{F}_{\text{P}\gamma^*\gamma^*}(-Q_1^2, -Q_2^2)$ , which can, in principle, be obtained from measurements.
- Relevant momentum regions from weight functions: below about 1 GeV for  $\pi^0$ , below about 1.5 GeV for  $\eta$  and  $\eta'$ .
- Showed impact of measurement errors of the doubly-virtual form factor on final result for  $a_{\mu}^{\text{HLbL};\text{P}}$  based on (preliminary) Monte-Carlo simulations for the signal of  $e^+e^- \rightarrow e^+e^-\gamma^*\gamma^* \rightarrow e^+e^-\text{P}$  at BES III. For illustration used two simple form factor models (LMD+V, VMD) for  $\pi^0$ , VMD for  $\eta, \eta'$ .
- With precision reachable for  $\mathcal{F}_{\text{P}\gamma^*\gamma^*}(-Q_1^2, -Q_2^2)$  from BES III in a few more years and with other input in particular at  $Q_{1,2} \leq 0.5$  GeV:

$$\delta a_{\mu}^{\text{HLbL};\pi^0} = 18\%$$

$$\delta a_{\mu}^{\text{HLbL};\eta} = 22\%$$

$$\delta a_{\mu}^{\text{HLbL};\eta'} = 15\%$$

- In order for the dispersive approach to HLbL to be successful, one needs the  $\pi^0, \eta^0, \eta'$ -pole contributions to 10% precision  $\Rightarrow$  needs to improve above uncertainties !
- Future: more work needed to estimate effect of backgrounds and analysis cuts at BES III. Further informations needed for form factor  $\mathcal{F}_{\text{P}\gamma^*\gamma^*}(-Q_1^2, -Q_2^2)$ , in particular for low  $Q_{1,2} \leq 1$  GeV from other experiments (KLOE 2 ? Belle 2 ?), from dispersion relations for form factor and maybe from Lattice QCD.

Backup slides

## HLbL scattering: Summary of selected results

Some results for the various contributions to  $a_{\mu}^{\text{HLbL}} \times 10^{11}$ :

Contribution	BPP	HKS, HK	KN	MV	BP, MdRR	PdRV	N, JN
$\pi^0, \eta, \eta'$	$85 \pm 13$	$82.7 \pm 6.4$	$83 \pm 12$	$114 \pm 10$	—	$114 \pm 13$	$99 \pm 16$
axial vectors	$2.5 \pm 1.0$	$1.7 \pm 1.7$	—	$22 \pm 5$	—	$15 \pm 10$	$22 \pm 5$
scalars	$-6.8 \pm 2.0$	—	—	—	—	$-7 \pm 7$	$-7 \pm 2$
$\pi, K$ loops	$-19 \pm 13$	$-4.5 \pm 8.1$	—	—	—	$-19 \pm 19$	$-19 \pm 13$
$\pi, K$ loops +subl. $N_C$	—	—	—	$0 \pm 10$	—	—	—
quark loops	$21 \pm 3$	$9.7 \pm 11.1$	—	—	—	$2.3$ (c-quark)	$21 \pm 3$
Total	$83 \pm 32$	$89.6 \pm 15.4$	$80 \pm 40$	$136 \pm 25$	$110 \pm 40$	$105 \pm 26$	$116 \pm 39$

BPP = Bijmans, Pallante, Prades '95, '96, '02; HKS = Hayakawa, Kinoshita, Sanda '95, '96; HK = Hayakawa, Kinoshita '98, '02; KN = Knecht, AN '02; MV = Melnikov, Vainshtein '04; BP = Bijmans, Prades '07; MdRR = Miller, de Rafael, Roberts '07; PdRV = Prades, de Rafael, Vainshtein '09; N = AN '09, JN = Jegerlehner, AN '09

- **Pseudoscalar-exchanges dominate numerically.** Other contributions not negligible. **Cancellation** between  $\pi, K$ -loops and quark loops !
- **PdRV:** Analyzed results obtained by different groups with various models and suggested new estimates for some contributions (shifted central values, enlarged errors). **Do not consider dressed light quark loops as separate contribution !** Assume it is already taken into account by using short-distance constraint of MV '04 on pseudoscalar-pole contribution. **Added all errors in quadrature !**
- **N, JN:** **New evaluation of pseudoscalar exchange contribution imposing new short-distance constraint on off-shell form factors.** Took over most values from BPP, except axial vectors from MV. **Added all errors linearly.**

# Expressions for weight functions $w_{1,2}(Q_1, Q_2, t)$

Jegerlehner, AN '09

$$w_1(Q_1, Q_2, t) = \left(-\frac{2\pi}{3}\right) \sqrt{1-t^2} \frac{Q_1^3 Q_2^3}{Q_2^2 + m_\pi^2} I_1(Q_1, Q_2, t)$$

$$w_2(Q_1, Q_2, t) = \left(-\frac{2\pi}{3}\right) \sqrt{1-t^2} \frac{Q_1^3 Q_2^3}{Q_3^2 + m_\pi^2} I_2(Q_1, Q_2, t)$$

$$I_1(Q_1, Q_2, t) = X(Q_1, Q_2, t) \left( 8 P_1 P_2 (Q_1 \cdot Q_2) - 2 P_1 P_3 (Q_2^4/m_\mu^2 - 2 Q_2^2) - 2 P_1 (2 - Q_2^2/m_\mu^2 + 2(Q_1 \cdot Q_2)/m_\mu^2) \right. \\ \left. + 4 P_2 P_3 Q_1^2 - 4 P_2 - 2 P_3 (4 + Q_1^2/m_\mu^2 - 2 Q_2^2/m_\mu^2) + 2/m_\mu^2 \right) \\ - 2 P_1 P_2 (1 + (1 - R_{m1})(Q_1 \cdot Q_2)/m_\mu^2) + P_1 P_3 (2 - (1 - R_{m1}) Q_2^2/m_\mu^2) + P_1 (1 - R_{m1})/m_\mu^2 \\ + P_2 P_3 (2 + (1 - R_{m1})^2 (Q_1 \cdot Q_2)/m_\mu^2) + 3 P_3 (1 - R_{m1})/m_\mu^2$$

$$I_2(Q_1, Q_2, t) = X(Q_1, Q_2, t) \left( 4 P_1 P_2 (Q_1 \cdot Q_2) + 2 P_1 P_3 Q_2^2 - 2 P_1 + 2 P_2 P_3 Q_1^2 - 2 P_2 - 4 P_3 - 4/m_\mu^2 \right) \\ - 2 P_1 P_2 - 3 P_1 (1 - R_{m2})/(2m_\mu^2) - 3 P_2 (1 - R_{m1})/(2m_\mu^2) - P_3 (2 - R_{m1} - R_{m2})/(2m_\mu^2) \\ + P_1 P_3 (2 + 3(1 - R_{m2}) Q_2^2/(2m_\mu^2) + (1 - R_{m2})^2 (Q_1 \cdot Q_2)/(2m_\mu^2)) \\ + P_2 P_3 (2 + 3(1 - R_{m1}) Q_1^2/(2m_\mu^2) + (1 - R_{m1})^2 (Q_1 \cdot Q_2)/(2m_\mu^2))$$

where  $Q_3^2 = (Q_1 + Q_2)^2$ ,  $Q_1 \cdot Q_2 = Q_1 Q_2 \cos \theta$ ,  $t = \cos \theta$

$$P_1^2 = 1/Q_1^2, \quad P_2^2 = 1/Q_2^2, \quad P_3^2 = 1/Q_3^2, \quad X(Q_1, Q_2, t) = \frac{1}{Q_1 Q_2 x} \arctan \left( \frac{zx}{1-zt} \right),$$

$$x = \sqrt{1-t^2}, \quad z = \frac{Q_1 Q_2}{4m_\mu^2} (1 - R_{m1})(1 - R_{m2}), \quad R_{mi} = \sqrt{1 + 4m_\mu^2/Q_i^2}$$

Form factor  $\mathcal{F}_{\pi^0\gamma^*\gamma^*}(q_1^2, q_2^2)$  and transition form factor  $F(Q^2)$

- Form factor  $\mathcal{F}_{\pi^0\gamma^*\gamma^*}(q_1^2, q_2^2)$  between an on-shell pion and two off-shell (virtual) photons:

$$i \int d^4x e^{iq_1 \cdot x} \langle 0 | T \{ j_\mu(x) j_\nu(0) \} | \pi^0(q_1 + q_2) \rangle = \varepsilon_{\mu\nu\alpha\beta} q_1^\alpha q_2^\beta \mathcal{F}_{\pi^0\gamma^*\gamma^*}(q_1^2, q_2^2)$$

$$j_\mu(x) = (\bar{\psi} \hat{Q} \gamma_\mu \psi)(x), \quad \psi \equiv \begin{pmatrix} u \\ d \\ s \end{pmatrix}, \quad \hat{Q} = \text{diag}(2, -1, -1)/3$$

(light quark part of electromagnetic current)

Bose symmetry:  $\mathcal{F}_{\pi^0\gamma^*\gamma^*}(q_1^2, q_2^2) = \mathcal{F}_{\pi^0\gamma^*\gamma^*}(q_2^2, q_1^2)$

Form factor for real photons is related to  $\pi^0 \rightarrow \gamma\gamma$  decay width:

$$\mathcal{F}_{\pi^0\gamma^*\gamma^*}(q_1^2 = 0, q_2^2 = 0) = \frac{4}{\pi\alpha^2 m_\pi^3} \Gamma_{\pi^0 \rightarrow \gamma\gamma}$$

Often normalization with chiral anomaly is used:

$$\mathcal{F}_{\pi^0\gamma^*\gamma^*}(0, 0) = -\frac{1}{4\pi^2 F_\pi}$$

- Pion-photon transition form factor:

$$F(Q^2) \equiv \mathcal{F}_{\pi^0\gamma^*\gamma^*}(-Q^2, q_2^2 = 0), \quad Q^2 \equiv -q_2^2$$

Note that  $q_2^2 = 0$ , but  $\vec{q}_2 \neq \vec{0}$  for on-shell photon !

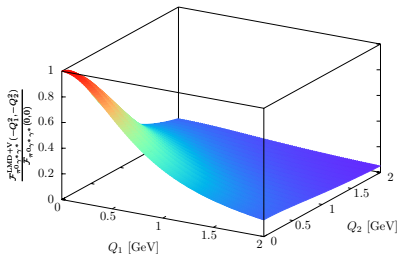
## Form factor model: LMD+V (large- $N_c$ QCD) versus VMD

For single-virtual FF, both models give equally good fit to CLEO data. Main difference: double-virtual case. VMD FF violates OPE, falls off too fast. For large  $Q^2$ :

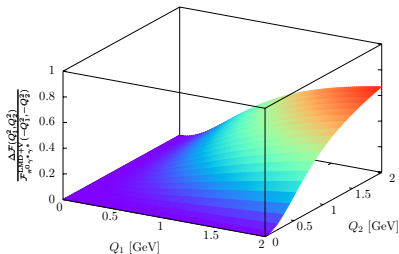
$$\mathcal{F}_{\pi^0\gamma^*\gamma^*}^{\text{LMD+V}}(-Q^2, -Q^2) \sim \mathcal{F}_{\pi^0\gamma^*\gamma^*}^{\text{OPE}}(-Q^2, -Q^2) \sim 1/Q^2 \quad \text{versus} \quad \mathcal{F}_{\pi^0\gamma^*\gamma^*}^{\text{VMD}}(-Q^2, -Q^2) \sim 1/Q^4$$

$$\text{Define: } \Delta\mathcal{F}(Q_1^2, Q_2^2) = \mathcal{F}_{\pi^0\gamma^*\gamma^*}^{\text{LMD+V}}(-Q_1^2, -Q_2^2) - \mathcal{F}_{\pi^0\gamma^*\gamma^*}^{\text{VMD}}(-Q_1^2, -Q_2^2)$$

$$\frac{\mathcal{F}_{\pi^0\gamma^*\gamma^*}^{\text{LMD+V}}(-Q_1^2, -Q_2^2)}{\mathcal{F}_{\pi^0\gamma^*\gamma^*}(0,0)}$$



$$\frac{\Delta\mathcal{F}(Q_1^2, Q_2^2)}{\mathcal{F}_{\pi^0\gamma^*\gamma^*}^{\text{LMD+V}}(-Q_1^2, -Q_2^2)}$$



$Q_1$ [GeV]	$Q_2$ [GeV]	$\frac{\mathcal{F}_{\pi^0\gamma^*\gamma^*}^{\text{LMD+V}}(-Q_1^2, -Q_2^2)}{\mathcal{F}_{\pi^0\gamma^*\gamma^*}(0,0)}$	$\frac{\mathcal{F}_{\pi^0\gamma^*\gamma^*}^{\text{VMD}}(-Q_1^2, -Q_2^2)}{\mathcal{F}_{\pi^0\gamma^*\gamma^*}(0,0)}$	$\frac{\Delta\mathcal{F}(Q_1^2, Q_2^2)}{\mathcal{F}_{\pi^0\gamma^*\gamma^*}^{\text{LMD+V}}(-Q_1^2, -Q_2^2)}$
0.5	0	0.707	0.706	0.0003
1	0	0.376	0.376	0.001
0.5	0.5	0.513	0.499	0.027
1	1	0.183	0.141	0.23

Since LMD+V and VMD FF differ for  $Q_1 = Q_2 = 1$  GeV by 23%, it might be possible to distinguish the two models experimentally at BES III, if binning is chosen properly.

# The LMD+V form factor

Knecht, AN, EPJC '01; AN '09

- Ansatz for  $\langle VVP \rangle$  and thus  $\mathcal{F}_{\pi^0\gamma^*\gamma^*}$  in large- $N_c$  QCD in chiral limit with 1 multiplet of lightest pseudoscalars (Goldstone bosons) and 2 multiplets of vector resonances,  $\rho, \rho'$  (lowest meson dominance (LMD) + V).
- $\mathcal{F}_{\pi^0\gamma^*\gamma^*}$  fulfills all leading and some subleading QCD short-distance constraints from operator product expansion (OPE).
- Reproduces Brodsky-Lepage (BL):  $\lim_{Q^2 \rightarrow \infty} \mathcal{F}_{\pi^0\gamma^*\gamma^*}(-Q^2, 0) \sim 1/Q^2$   
(OPE and BL cannot be fulfilled simultaneously with only one vector resonance).
- Normalized to decay width  $\Gamma_{\pi^0 \rightarrow \gamma\gamma}$

$$\mathcal{F}_{\pi^0\gamma^*\gamma^*}^{\text{LMD+V}}(q_1^2, q_2^2) = \frac{F_\pi}{3} \frac{q_1^2 q_2^2 (q_1^2 + q_2^2) + h_1 (q_1^2 + q_2^2)^2 + \bar{h}_2 q_1^2 q_2^2 + \bar{h}_5 (q_1^2 + q_2^2) + \bar{h}_7}{(q_1^2 - M_{V_1}^2)(q_1^2 - M_{V_2}^2)(q_2^2 - M_{V_1}^2)(q_2^2 - M_{V_2}^2)}$$

$F_\pi = 92.4$  MeV,  $M_{V_1} = M_\rho = 775.49$  MeV,  $M_{V_2} = M_{\rho'} = 1.465$  GeV

Free model parameters:  $h_i, \bar{h}_i$

Transition form factor:

$$F^{\text{LMD+V}}(Q^2) = \frac{F_\pi}{3} \frac{1}{M_{V_1}^2 M_{V_2}^2} \frac{h_1 Q^4 - \bar{h}_5 Q^2 + \bar{h}_7}{(Q^2 + M_{V_1}^2)(Q^2 + M_{V_2}^2)}$$

- $h_1 = 0$  GeV<sup>2</sup> (Brodsky-Lepage behavior  $\mathcal{F}_{\pi^0\gamma^*\gamma^*}^{\text{LMD+V}}(-Q^2, 0) \sim 1/Q^2$ )
- $\bar{h}_2 = -10.63$  GeV<sup>2</sup> (Melnikov, Vainshtein '04: Higher twist corrections in OPE)
- $\bar{h}_5 = 6.93 \pm 0.26$  GeV<sup>4</sup> -  $h_3 m_\pi^2$  (fit to CLEO data of  $\mathcal{F}_{\pi^0\gamma^*\gamma^*}^{\text{LMD+V}}(-Q^2, 0)$ )
- $\bar{h}_7 = -\frac{N_c M_{V_1}^4 M_{V_2}^4}{4\pi^2 F_\pi^2} = -14.83$  GeV<sup>6</sup> (or normalization to  $\Gamma(\pi^0 \rightarrow \gamma\gamma)$ )

# The VMD form factor

Vector Meson Dominance:

$$\mathcal{F}_{\pi^0 \gamma^* \gamma^*}^{\text{VMD}}(q_1^2, q_2^2) = -\frac{N_c}{12\pi^2 F_\pi} \frac{M_V^2}{q_1^2 - M_V^2} \frac{M_V^2}{q_2^2 - M_V^2}$$

Only two model parameters:  $F_\pi$  and  $M_V$

Note:

- VMD form factor **factorizes**  $\mathcal{F}_{\pi^0 \gamma^* \gamma^*}^{\text{VMD}}(q_1^2, q_2^2) = f(q_1^2) \times f(q_2^2)$ . This might be a too simplifying assumption / representation.
- VMD form factor has **wrong short-distance behavior**:  $\mathcal{F}_{\pi^0 \gamma^* \gamma^*}^{\text{VMD}}(q^2, q^2) \sim 1/q^4$ , for large  $q^2$ , **falls off too fast** compared to OPE prediction  $\mathcal{F}_{\pi^0 \gamma^* \gamma^*}^{\text{OPE}}(q^2, q^2) \sim 1/q^2$ .

Transition form factor:

$$F^{\text{VMD}}(Q^2) = -\frac{N_c}{12\pi^2 F_\pi} \frac{M_V^2}{Q^2 + M_V^2}$$